GLIA 55:1348–1361 (2007)

Multiple Cascade Effects of Oxidative Stress on Astroglia

CHERIE E. BOND AND SUSAN A. GREENFIELD
Department of Pharmacology, University of Oxford, Oxford OX1 3QT, United Kingdom

KEY WORDS
RNA; acetylcholinesterase; calcium; L-VGCC; TRPM2; protein; rat; calcium channels

ABSTRACT
Many neurodegenerative diseases share common underlying features, most prominent of which are dysregulation of calcium homeostasis and reactive astrogliosis, ultimately triggered by oxidative stress. Interestingly, an additional feature of the early response to stress conditions is the upregulation and release of acetylcholinesterase (AChE). This study therefore investigates the link between oxidative stress, calcium influx, gene expression, protein synthesis, and AChE release. We report that, in astroglia and in an immortalized cell line, GH4-hα7, acute oxidative stress causes influx of extracellular calcium through L-type voltage-gated calcium channels (L-VGCC), followed by increased release of AChE into the extracellular medium. Moreover, rapid and sustained changes in mRNA expression of AChE, L-VGCC, and melastatin-like transient receptor potential 2 (TRPM2) accompany profound suppression of global protein synthesis. Application of L-VGCC blockers selectively reduces stress-induced calcium influx and AChE release, mitigates changes in gene expression, and facilitates recovery from protein synthesis suppression. Although glia exhibit greater sensitivity in their responses, the results are comparable in astroglia and GH4-hα7 cells, and suggest a generalized and integrated cellular response to stress conditions that characterizes changes observed in neurodegeneration.

INTRODUCTION

Alzheimer's disease, Parkinson's disease, and amyotrophic lateral sclerosis, the three most common neurodegenerative disorders, display overlapping pathologies, (Greenfield and Vaux, 2002) and share distinct features with other rarer neurodegenerative diseases, such as Huntington's disease (Browne and Beal, 2006). The hallmark features characterizing the diverse range of neurodegenerative diseases suggest an underlying common mechanism. Oxidative stress induces the increased production of reactive oxygen species (ROS), which at low levels are important for neuronal development and signaling, but at higher levels appear to be a causative factor in neurodegeneration (Mariani et al., 2005; Markesbery and Lovell, 2006). Excessive oxidation damages nucleic acids, proteins, and lipids, disrupting mitochondrial energy metabolism, and causing increased calcium influx across the plasma membrane (Sultana et al., 2006). Calcium-dependent release of neurotrophic factors and cytokines by astroglia in response to oxidative stress initiates signaling cascades that, in the developing brain, eventually result in selective differentiation or apoptosis of cell lineages (Mattson, 2006; Morale et al., 2006). However, in the aged brain, where regulation of ROS is impaired (Norris et al., 1998), high levels of $[Ca^{2+}]_i$ become excitotoxic and lead to reactive astrogliosis (Marchetti et al., 2005), cell death (Alberdi et al., 2005; Eimerl and Schramm, 1994), and neurodegeneration (Greenfield and Vaux, 2002).

It is now well established that acetylcholinesterase (AChE, EC 3.1.1.7) is an important trophic factor in neurodevelopment (Coleman and Taylor, 1996; Dori et al., 2005; Sharma et al., 2001; Whyte and Greenfield, 2003), and in cellular stress responses (Kaufer et al., 1998; Pick et al., 2004). In particular, alternatively spliced 3′-isoforms of the AChE molecule correlate with opposing determinants of neuronal fate (Sternfeld et al., 2000). The "readthrough" form (R-AChE), specifically, is upregulated in response to many forms of stress, including psychological stress (Pick et al., 2004), ischemia/stroke, and head injury (Shohami et al., 1999). Moreover, we have demonstrated recently that transcription and release of R-AChE by reactive astroglia is increased in response to oxidative stress (Bond et al., 2006).

The trophic action of AChE (Day and Greenfield, 2002) and astroglial release of neurotrophic factors (Vaca and Wendt, 1992) are dependent on $[Ca^{2+}]$ entry through L-VGCC. Since L-VGCC have been shown to specifically mediate neuronal excitation-transcription coupling (Zhang et al., 2006), we have investigated the role of these calcium channels in regulating AChE release and changes in transcription and translation in astroglia in response to oxidative damage. In addition, recent studies have shown that ROS activate the neuronal TRPM2 channel, leading to sustained increases in $[Ca^{2+}]_i$ and cell death (Fonfria et al., 2004). This proposed sensor of cellular redox status, highly expressed in microglia, is generally absent in astroglia (Kraft et al., 2004). However, astroglia are known to alter their receptor and ion channel complement to adapt to local environmental changes (Porter and McCarthy, 1997; Verkhratsky et al., 1998). Thus, we also examined the

Grant sponsor: Synaptica, Ltd.; The James Martin 21st Century School Foundation.

*Correspondence to: Dr. Cherie E. Bond, Department of Pharmacology, University of Oxford, Mansfield Road, Oxford OX1 3QT, UK.
E-mail: cherie.bond@pharm.ox.ac.uk

Received 16 April 2007; Revised 6 June 2007; Accepted 18 June 2007

DOI 10.1002/glia.20547

Published online 25 July 2007 in Wiley InterScience (www.interscience.wiley.com).

effects of oxidative stress on astroglial TRPM2 expression and the consequences of TRPM2-mediated calcium influx.

MATERIALS AND METHODS

All reagents were purchased from Sigma-Aldrich, Poole, UK, unless otherwise noted. Verapamil, nimodipine, nifedipine, ω-conotoxin MVIIC, and DHBP were purchased from Tocris Cookson, Bristol, UK. Disposables and cell culture plasticware were from Fisher Scientific, Loughborough, UK.

Preparation of Astroglia and Cell Culture Methods

Astroglia were prepared as previously described (Whyte and Greenfield, 2003). Briefly, P1-P3 Wistar rats were treated with an overdose of isofluorane anaesthetic (Schedule 1, Animal Scientific Procedures Act, UK, 1986), and then decapitated in a sterile environment. The cerebrum was removed by blunt dissection, rolled on sterile filter paper to remove meninges, cut into ~1 mm^3 pieces, and dissociated with gentle trituration in Dulbecco's modified Eagle's medium with 4,500 mg/L glucose and GlutaMAX (DMEM; Life Technologies Ltd., Paisley, UK) containing 10% fetal calf serum, 100 units/mL penicillin, 100 μg/mL streptomycin, and 2.5 μg/mL amphotericin B. The dissociated tissue was plated into 75-cm^2 flasks precoated with poly-D-lysine (PDL), then incubated at 37°C in a humidified atmosphere (95% air: 5% CO_2) for 7 days. Before passaging, confluent flasks were agitated on a shaking platform to dislodge any contaminating microglia adhering to the astroglial monolayer. Microglia collected were washed and centrifuged to pellet, then lysed and processed for RNA extraction. Astroglia were washed with 1× Hanks balanced salt solution (HBSS), lifted with 1× trypsin, placed into clean PDL-coated 75-cm^2 flasks and allowed to reach confluency. Astroglia were again passaged into clean PDL-coated flasks or 6-well plates and allowed to recover for 1–3 days before experimentation. Identification of the cultures as Type 1 reactive astrocytes was confirmed by microscopic examination of morphology and immunocytochemical detection with a glial fibrillary acidic protein antibody (>99% positive). To reduce inter-animal variability, each experiment using astroglia was performed on a pool of astrocytes derived from the cortices of ~20 pups from two litters.

GH4-hα7 cells (Merck & Co, Rahway, USA) were maintained in DMEM (4,500 mg/L glucose with GlutaMAX) containing 10% fetal bovine serum, 100 units/mL penicillin, 100 μg/mL streptomycin, 2.5 μg/mL amphotericin B, and 500 μg/mL active G418 (geneticin). Ca^{2+}-free, serum-free media was prepared with calcium-free DMEM (4,500 mg/mL glucose; Invitrogen, Paisley, UK), 25 mM HEPES, 2 mM GlutaMAX (Invitrogen, Paisley, UK), 100 units/mL penicillin, 100 μg/mL streptomycin, 2.5 μg/mL amphotericin B, and 1.8 mM $BaCl_2$. Medium was sterilized by filtration through a 0.22 μm polyethersulfone low protein binding membrane and stored at 4°C.

Treatment with *t*-BHP and Drugs

Confluent astroglia and GH4 cells were seeded into 6-well plates at a density of 1×10^5 cells/well and allowed to recover for 1–2 days, until cells were about 90% confluent. Cells were conditioned overnight in serum-free DMEM, then *tert*-butyl hydroperoxide (*t*-BHP) in serum-free medium or control serum-free medium was added to the cells in the presence or absence of various calcium channel blockers for 1 h. On the basis of preliminary experiments, the optimal concentration of *t*-BHP to elicit a measurable AChE response, without inducing significant cell death, was 100–500 μM for astroglia and GH4 cells. Media was removed and cells were washed twice with 2 mL serum-free DMEM to remove residual *t*-BHP, then 1 mL serum-free medium was added to each well and cells were incubated at 37°C for 1 h before sampling medium for released AChE activity.

Stock solutions of nifedipine and nimodipine were prepared in sterile dimethylsulfoxide (DMSO); all other stock drug solutions were prepared in sterile water. Stock solutions were stored at −20°C and diluted at least 1,000-fold in assay buffer or culture media before use. The final concentration of DMSO in treatment medium was less than 0.01%. Treatment of control cultures with this concentration of DMSO alone had no effect on cell viability, AChE release, gene expression, intracellular calcium levels, or protein synthesis. Because there is currently no pharmacological agent available to specifically inhibit TRPM2, an indirect method was used. Benzamide is a potent inhibitor of the nuclear enzyme poly-adenosine diphosphate polymerase (PARP-1) that is activated by DNA damage induced by oxidative stress. TRPM2 activation is dependent on phosphorylation of ADP-ribose generated by PARP-1 activity and PARP-1 inhibitors have been shown to block TRPM2 activation (Fonfria et al., 2004).

Measurement of Cholinesterase Activity

The method of Ellman et al. (1961) was used to determine the levels of cholinesterase released into media samples. Briefly, media was removed from the cells at various time intervals, centrifuged, and 25 μL aliquots were taken from the supernatant for analysis. To ensure that observed esterase activity was exclusively attributable to AChE, rather than the alternative esterase butyrylcholinesterase (BuChE), samples were assayed in the presence of the specific BuChE antagonist tetra-isopropyl pyrophosphoramide (Iso-OMPA, 100 μM). Absorbance was read at 405 nm over 20 min using a Molecular Devices plate reader (Alpha Laboratories, Hampshire, UK). Baseline control values from cell media were subtracted from appropriate experimental values. AChE ac-

tivity was calculated (V_{max} × enzyme efficiency factor × dilution factor = mU/mL/min) and statistical analyses were performed by ANOVA, followed by appropriate *post hoc* tests, using GraphPad Prism 4 data analysis program (GraphPad Software, San Diego, USA).

Intracellular Calcium Assays

Calcium assays were performed using a Fluo-4 NW calcium assay kit (Molecular Probes, Invitrogen, Paisley, UK) as per the manufacturer's recommendations for adherent cells. Briefly, cells were seeded into a poly-D-lysine-coated black, flat-bottom, 96-well plate (Greiner Bio-One Ltd, Stonehouse, UK) at a density of 1×10^4 cells/well and allowed to recover for 24 h. Cell growth media was removed and cells were washed with 200 μL/well assay buffer (20 mM HEPES in 1× HBSS). One hundred microliters of freshly prepared dye loading solution was added to each well and plates were incubated in the dark, at 37°C for 30 min, then at 25°C for an additional 30 min. Drug dilutions and *t*-BHP were prepared in assay buffer at 3-fold final concentrations, then, immediately prior to measurement, 50 μL aliquots were added to the appropriate wells of the plate. Fluorescence was measured on a NOVOstar microplate fluorometer (BMG Labtech, Ayesbury, UK) using excitation filter 485DF12 and emission filter 520DF35. Fluorescence measurements were acquired at ~1 min intervals for 1 h, then drugs were washed out and measurements were continued at the same rate for a second hour. Finally, measurements were obtained every 5 min for 8 h. Relative fluorescence was calculated by averaging six baseline-subtracted measurements at each time point acquired for each treatment.

Total RNA Isolation, cDNA Preparation, and PCR Amplification

Total RNA was isolated from astroglial and GH4 cells using the Sigma GenElute™ Mammalian Total RNA kit. RNA was reverse transcribed into cDNA using SuperScript First-Strand Synthesis System (Invitrogen, Paisley, UK) as per the manufacturer's instructions. Briefly, 2 μg total RNA was annealed with 50 ng random hexamers and dNTP mix, then remaining reaction components were added to a final volume of 20 μL. Reactions were incubated at 42°C for 50 min, terminated at 70°C, and then RNA was removed by incubation with RNase H for 20 min at 37°C. One hundred nanograms cDNA was amplified by PCR with 50 pmol gene-specific primers, 1.5 mM $MgCl_2$, 200 μM dNTPs, and 1.25 U Taq DNA polymerase (Promega, Southampton, UK) in a 50 μL final reaction volume. After an initial denaturation of 95°C for 2 min, reactions were amplified for 35 cycles: 95°C for 30 s, 55°C for 30 s, 72°C for 1 min, followed by a final extension of 72°C for 10 min. Reaction products were separated by electrophoresis on 1.5–2.0% agarose TAE gels and visualized by UV illumination. Images were captured and band density determined using a Bio-Rad Gel Doc 2000 and QuantityOne software (Bio-Rad, Hempstead, UK). Relative band density was determined by calculating the ratio of specific gene band density to GAPDH band density for each sample. Values from three separate experiments were averaged and statistical significance was determined by ANOVA followed by *post hoc* multiple comparison Bonferroni test.

Determination of Protein Synthesis Levels

The effect of oxidative stress on overall protein synthesis was evaluated on cultures. Briefly, confluent cell layers were lifted, washed, and replated into 6-well cell culture dishes (precoated with poly-D-lysine for astroglia) at a density of 1×10^5 cells/well. Cells were allowed to recover for 1–2 days, until about 90% confluent, conditioned overnight in serum-free medium, and then stressed with 200 μM *t*-BHP in serum-free medium for 1 h in the presence or absence of various calcium channel blockers. The cultures were washed three times with cell medium to remove residual *t*-BHP and drugs. Fresh cell medium was applied containing 15 μCi/mL [^{3}H]-leucine (Amersham Biosciences, Chalfont St. Giles, UK) 6 h before harvesting cells for analysis. After 6, 24, or 72 h, the medium fractions were collected and brought to 10% trichloroacetic acid (TCA) concentration. The culture dishes were washed with HBSS and the cell layers were harvested by scraping into 10% cold TCA. Medium and cell fractions were combined and incubated for 24 h at 4°C. Protein precipitates were collected and washed by rapid filtration through Whatman GFB filters, using a Brandel cell harvester (SEMAT Technical, St. Albans, UK). The filters were placed in scintillation vials containing 5 mL Ecoscint H scintillation fluid, allowed to shake overnight at 200 rpm, and then radioactivity was determined in a liquid scintillation counter (Beckman LS60001C, Beckman Coulter, High Wycombe, UK).

RESULTS

The Role of Calcium in Oxidative Stress-Induced Morphological Changes and AChE Release

During exposure to *t*-BHP, astroglia showed no significant change in AChE release or overt phenotypic changes as determined by microscopic examination. However, during the poststress recovery period, striking morphological changes became apparent (Fig. 1A, a/b). The severity and rapidity of this response was dependent on the concentration of *t*-BHP applied. Perforations in the cell monolayer were observed within 1 h of recovery from *t*-BHP-induced oxidative stress, because of retraction of cell processes, condensation of cell bodies, and cell detachment from the plates. In addition, numerous inclusion bodies and vacuoles were observed in the cytoplasm of treated cells. Astroglia exposed to high levels of *t*-BHP (>0.5 mM) in the presence of extracellular

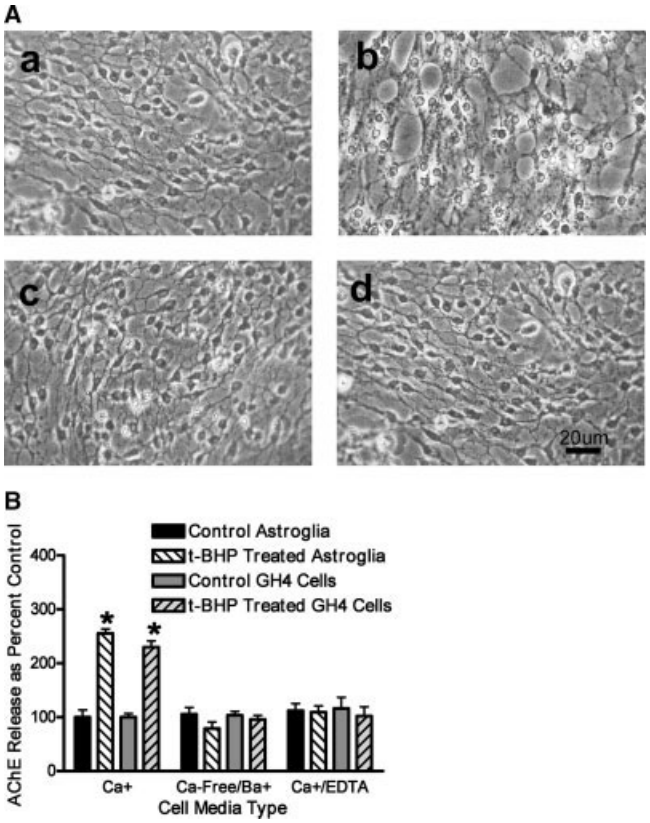

Fig. 1. Effect of extracellular calcium influx on astroglial response to oxidative stress. **A**: Phase contrast micrographs of live astrocytes in culture. Panel a: Control astroglia in serum-free medium containing $CaCl_2$. Panel b: Astroglia treated for 1 h with 1.0 mM *t*-BHP in serum-free medium with $CaCl_2$, followed by 1 h recovery period. Panel c: Control astroglia in serum-free medium with $BaCl_2$ substituted for $CaCl_2$. Panel d: *t*-BHP-treated astroglia in serum-free medium with $BaCl_2$.substituted for $CaCl_2$. (Magnification = 20×) **B**: Substituting $BaCl_2$ for $CaCl_2$ in the cell growth medium or chelating extracellular calcium with 1 mM EDTA abolished induced AChE release from both astroglia and GH4 cells. Cells were exposed to 0.5 mM *t*-BHP treatment for 1 h followed by recovery in serum-free medium for 1 h. Asterisks indicate values significantly different from controls ($n = 9, P < 0.001$).

calcium did not recover, but continued to degenerate over the course of the following week and eventually all died. In contrast, those exposed to lower levels of *t*-BHP (0.1–0.5 mM) exhibited dose-dependent phenotypic changes and recovery. These profound phenotypic changes were completely abolished, even at the highest concentration of *t*-BHP tested, by eliminating extracellular Ca^{2+} from the culture medium (Fig. 1A, c/d). In contrast to the findings in astroglia, GH4 cells stressed with 0.1–1.0 mM *t*-BHP did not exhibit any apparent morphological changes indicative of apoptosis, although cells became less adherent during the recovery period. Signs of necrotic cell death were observed at *t*-BHP treatment concentrations over 0.5 mM, including cell swelling, cell detachment from plates, and rupture of cell membranes over a 24 h recovery period poststress.

After 1 h recovery from oxidative stress, astroglial release of AChE increased more than 2-fold (255.56% ± 8.38%) as compared with unstressed glia controls (Fig. 1B). A similar increase in AChE activity was observed in GH4 cells after exposure to *t*-BHP (229.71% ± 11.87%) as compared with GH4 controls. Elimination of Ca^{2+} from the extracellular medium abolished the *t*-BHP-induced release of AChE from astroglia. Basal AChE release from astroglia and GH4 cells was not significantly affected by substitution of Ba^{2+} for Ca^{2+}, or by chelation of Ca^{2+} by EDTA, in the extracellular medium.

Regulation of Stress-Induced AChE Release and Morphological Changes by Calcium Channels

AChE levels were measured in media from cells exposed to *t*-BHP in the presence and absence of various calcium channel inhibitors. The compiled results of AChE activity assays are summarized in Table 1. Basal AChE release from astroglia was significantly reduced by the L-VGCC blockers, verapamil (33% of control val-

TABLE 1. Effect of Calcium Channel Blockers on Oxidative Stress-Induced AChE Release from Astroglia and GH4-hα7 Cells

	Control			*t*-BHP stressed			
	Mean (mU/ml)	SEM	*P* vs. control	Mean (mU/ml)	SEM	*P* vs. control	*P* vs. stressed
Astroglia							
No drug	0.90	0.12	–	2.47	0.28	0.0004	–
Verapamil	0.30	0.11	0.004	1.06	0.15	0.424	0.001
Nimodipine	0.37	0.12	0.036	1.26	0.33	0.329	0.019
Nifedipine	0.49	0.12	0.013	1.17	0.34	0.471	0.015
Conotoxin	0.23	0.10	0.002	1.95	0.12	0.0001	0.119
DHBP	0.18	0.10	0.001	1.58	0.23	0.025	0.034
Benzamide	0.88	0.13	0.912	2.36	0.22	0.0002	0.764
Benza + verap	0.29	0.12	0.005	1.01	0.18	0.622	0.001
GH4 Cells							
No drug	2.76	0.52	–	6.34	0.53	0.008	–
Verapamil	2.72	0.48	0.762	4.18	0.44	0.051	0.011
Nimodipine	2.78	0.34	0.487	4.11	0.58	0.152	0.018
Nifedipine	2.83	0.45	0.784	3.54	0.68	0.588	0.009
Conotoxin	2.22	0.43	0.466	4.88	0.46	0.077	0.064
DHBP	1.99	0.28	0.259	6.45	0.46	0.003	0.903
Benzamide	2.57	0.44	0.786	6.39	0.49	0.001	0.946
Benza + verap	2.51	0.38	0.695	3.99	0.52	0.125	0.010

Cells were stressed with 0.5 mM *t*-BHP for 1 h in the presence and absence of calcium channel blockers, and then allowed to recover for 1 h before sampling medium for AChE activity. Experiments were performed twice in triplicate. Data shown are expressed as mU/ml/min. Statistical analyses were performed by 2-way ANOVA for overall determination of stress effect (50% of total variance, $P < 0.0001$), drug effect (16% of total variance, $P < 0.0001$), and interaction between stress and drug effects (6% of total variance, $P = 0.036$). Unpaired *t*-tests were used to determine significant differences of individual drug effects compared with no drug control and drug + stress effects versus no drug stressed values.

ues), nimodipine (41%), and nifedipine (54%); the N/P/Q-VGCC blocker ω-conotoxin MVIIC (25%); and the ryanodine receptor inhibitor DHBP (20%), but not by the poly-adenosine diphosphate polymerase (PARP-1) inhibitor benzamide. In contrast to the results seen in astroglia, GH4 cell basal AChE release was not affected by any of the calcium channel blockers tested.

After treatment with *t*-BHP, AChE release increased more than 2-fold in astroglia and GH4 cells. This increased release was significantly inhibited in both cell lines by verapamil, nimodipine, and nifedipine, but not by ω-conotoxin MVIIC or benzamide. DHBP reduced AChE release in *t*-BHP-stressed astroglia, but not in GH4 cells. L-VGCC blockers coapplied with *t*-BHP treatment significantly mitigated obvious morphological changes in astroglia in the initial poststress recovery period. Although glia exhibited some process retraction and condensation, fewer cytoplasmic inclusion bodies were observed and cells remained adherent. DHBP, ω-conotoxin MVIIC, and benzamide alone had no effect on observed stress-induced morphological changes in glia.

Because the measured AChE release from stressed cells can include both basal and *t*-BHP-induced AChE release, the effect on induced release attributed to different calcium channel blockers could be obscured by drug effects on basal release. When the observed basal release for each drug treatment was subtracted from the total release under *t*-BHP stress, the actual drug effect on induced release was revealed. In astroglia and GH4 cells, only L-VGCC blockade significantly inhibited induced AChE release (Figs. 2A,B). DHBP and ω-conotoxin had no effect on induced AChE release in either cell type. When GH4 cells were treated with verapamil in a concentration range of 10 pM to 10 μM, a distinct concentration dependent inhibition of AChE release was observed in *t*-BHP stressed cells (EC50 = 2.5 nM, Fig. 2C). Comparison of normalized EC50 values (control = 3.48 nM and *t*-BHP = 3.31 nM) and Hill coefficients (−0.56 and −0.64 respectively) verified that *t*-BHP treatment did not alter verapamil efficacy or potency to effect AChE release inhibition.

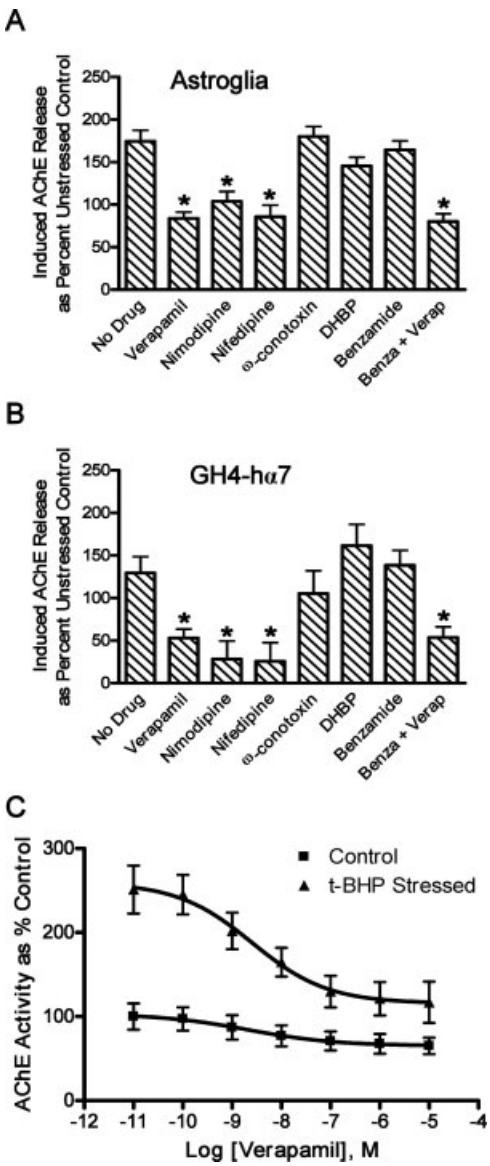

Fig. 2. Effect of calcium channel blockers on oxidative stress-induced AChE release. **A**: Astroglia were exposed to 0.5 mM *t*-BHP for 1 h in the presence and absence of verapamil, nimodipine, and nifedipine (10 μM), ω-conotoxin MVIIC (100 nM), DHBP (10 μM), and benzamide (100 μM). Cells were recovered for 1 h, and then medium was sampled and assayed for AChE activity using the method of Ellman et al. (1961). All AChE measurements were performed in triplicate. Results shown were calculated by subtracting average control (basal) from *t*-BHP-stressed (basal + induced) AChE levels for each drug treatment, then expressed as % unstressed, no drug control to reveal actual changes in induced AChE release. Data were analyzed by ANOVA, followed by comparison of means by unpaired *t*-test. Asterisks indicate values significantly different from controls, $P < 0.005$, $n = 6$. **B**: GH4-hα7 cells were exposed to 0.5 mM *t*-BHP in the presence and absence of indicated calcium channel blockers as described above. Data were analyzed and displayed as above. Asterisks indicate values significantly different from controls, $P < 0.007$, $n = 6$. **C**: Dose response curve of GH4-hα7 cells stressed with 0.5 mM *t*-BHP in the presence of indicated verapamil concentrations. Data were expressed as % unstressed control and analyzed by nonlinear regression with variable slope (Goodness of fit $R^2 = 0.997$) followed by two-tailed paired *t*-test (means significantly different, $n = 3$, $P < 0.002$).

Calcium Channel Regulation of Extracellular Ca^{2+} Influx During Oxidative Stress

Application of 100 μM *t*-BHP for 1 h to astroglia and GH4 cells resulted in increased intracellular Ca^{2+} during the treatment period (Fig. 3). Initiation of accelerated calcium influx was delayed for about 20 min in astroglia (Fig. 3A), whereas increasing calcium accumulation was observed immediately in GH4 cells (Fig. 3D). In the presence of verapamil, the effect of *t*-BHP on cumulative $[Ca^{2+}]_i$ was abolished in both cell lines (Figs. 3A,D). After the initial nonresponsive period, calcium levels in astroglia climbed sharply, rapidly surpassing levels seen in GH4 cells. The maximum rate of change in $[Ca^{2+}]_i$ increased 4-fold in astroglia exposed to *t*-BHP ($P < 0.001$; Fig. 3B), resulting in a 200% increase in average rate of change in $[Ca^{2+}]_i$ in stressed cells as com-

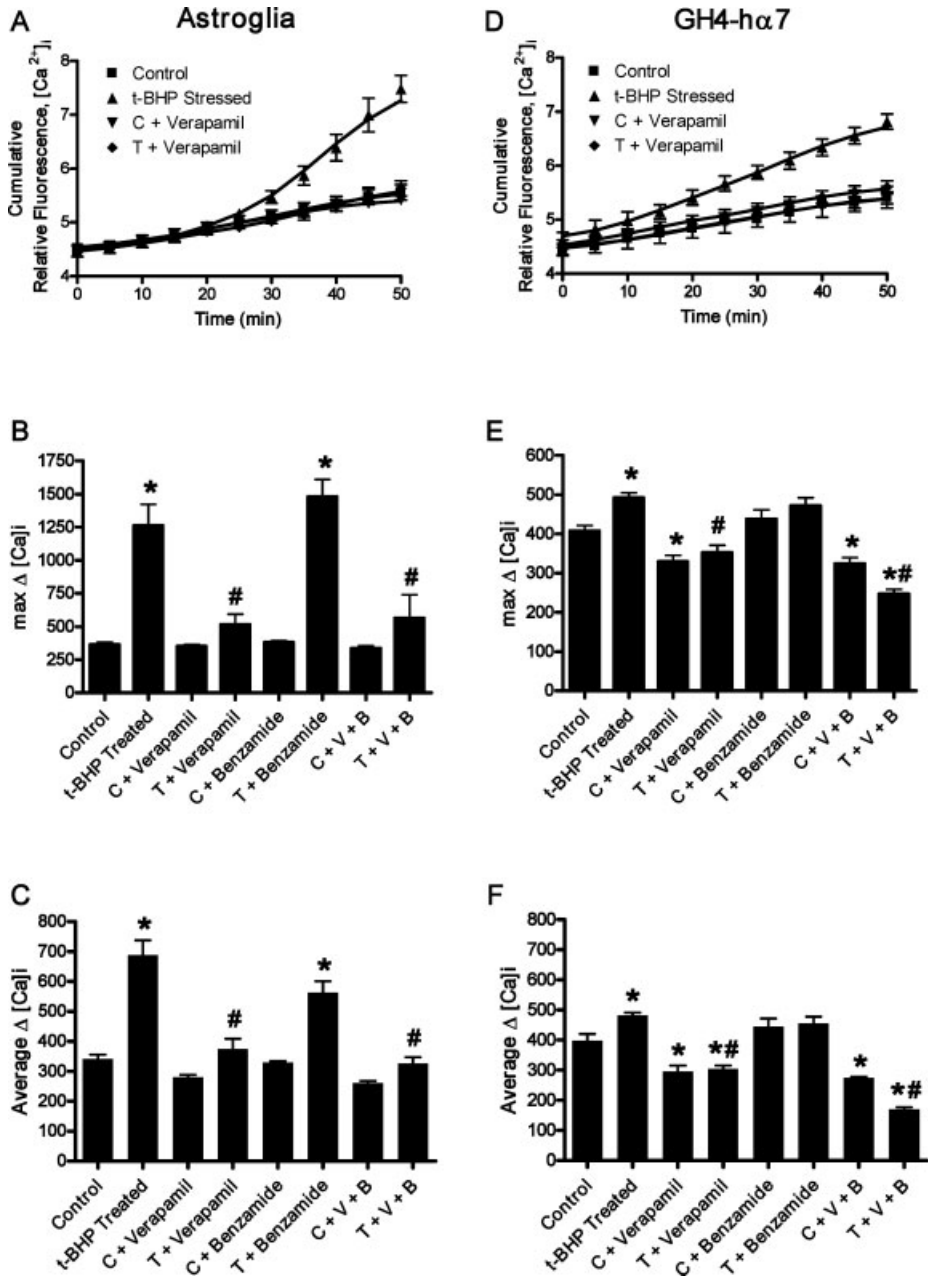

Fig. 3. Changes in $[Ca^{2+}]_i$ in response to 100 μM *t*-BHP treatment for 1 h. Results obtained from astroglia are shown in the left panels; results from GH4 cells are on the right. **A**: Cumulative $[Ca^{2+}]_i$ fluorescence was measured in cells at ~1 min intervals during exposure to oxidative stress in the absence and presence of verapamil. Values shown are the average measurements (mean ± SEM) of six replicate treatment samples recorded at 5 min intervals throughout the treatment period. **B**: Maximum change in $[Ca^{2+}]_i$ was determined by first calculating the difference in $[Ca^{2+}]_i$ between consecutive measurements for each sample, then the differences from six replicate treatment samples were averaged and expressed as mean ± SEM relative fluorescence units (RFU). The maximum change observed for each treatment group is displayed. **C**: Average change in $[Ca^{2+}]_i$ was determined by first calculating the average differences between consecutive measurements across the entire treatment period for each sample. Data shown are the mean ± SEM RFU obtained by averaging replicate treatment sample values. Asterisks (*) indicate values significantly different from unstressed, no drug controls; (#) indicates values from cells stressed in presence of drugs that are significantly different from *t*-BHP-stressed controls. Abbreviations: C = control, T = *t*-BHP treated, V = verapamil (10 μM), B = benzamide (100 μM).

pared with controls ($P < 0.001$; Fig. 3C). Neither verapamil nor benzamide had any effect on $[Ca^{2+}]_i$ in control astroglia. In contrast, *t*-BHP-induced increases in maximum and average rates of $[Ca^{2+}]_i$ accumulation were reduced to control levels in the presence of verapamil ($P < 0.001$). Benzamide alone had no significant effect on *t*-BHP-induced $[Ca^{2+}]_i$ changes in astroglia. Similarly, benzamide applied in combination with verapamil had no further effect on *t*-BHP-induced $[Ca^{2+}]_i$ changes over that of verapamil alone (Figs. 3B,C).

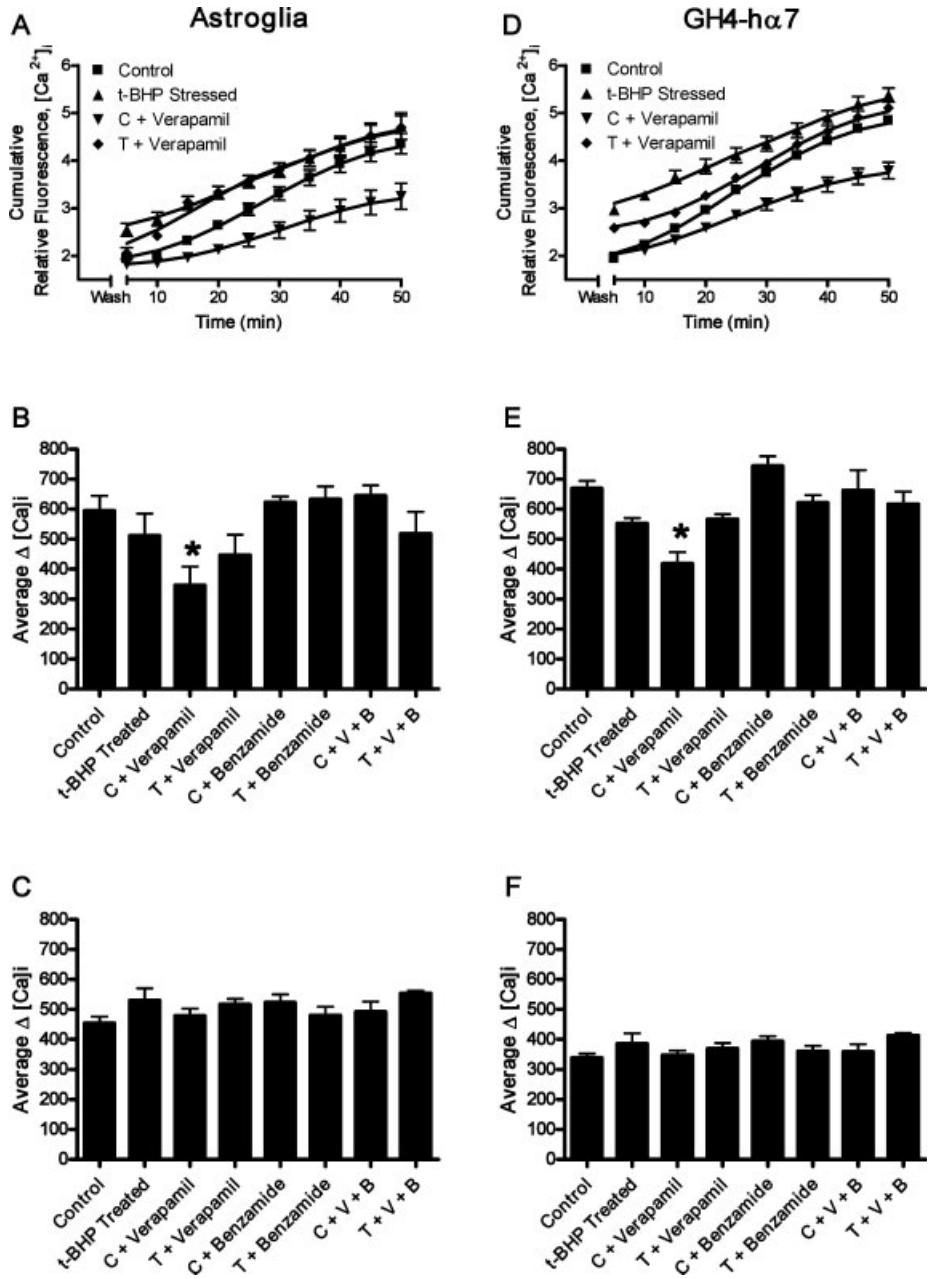

Fig. 4. Changes in $[Ca^{2+}]_i$ in the poststress recovery period. Results obtained from astroglia are shown in the left panels; results from GH4 cells are on the right. **A**: Cumulative $[Ca^{2+}]_i$ fluorescence measured in cells for 1 h after washout of drugs and *t*-BHP. Values shown are the average (mean ± SEM) of 6 replicate treatment samples recorded at 5 min intervals during the initial recovery period. **B**: Average change in $[Ca^{2+}]_i$ throughout the initial 1 h recovery period. **C**: Average change in $[Ca^{2+}]_i$ during the subsequent 8 h recovery period. Abbreviations: C = control, T = *t*-BHP treated, V = verapamil (10 μM), B = benzamide (100 μM).

Although changes in $[Ca^{2+}]_i$ were apparent in GH4 cells immediately upon exposure to oxidative stress, the observed increase was more gradual than that seen in astroglia (Fig. 3D). Maximum and average rates of change in $[Ca^{2+}]_i$ showed modest but significant ($P < 0.05$) increases in *t*-BHP-treated GH4 cells (Figs. 3E,F). As was seen in astroglia, verapamil effectively abolished *t*-BHP-induced $[Ca^{2+}]_i$ increases ($P < 0.001$), whereas benzamide alone had no effect. However, coapplication of verapamil and benzamide with *t*-BHP further suppressed maximum and average change in $[Ca^{2+}]_i$ as compared with the effect of verapamil alone ($P < 0.001$; Figs. 3E,F). In contrast to results in astroglia, verapamil also significantly depressed maximum ($P < 0.05$) and average ($P < 0.01$) $[Ca^{2+}]_i$ changes in control GH4 cells.

Ca^{2+} Influx During Poststress Recovery

To follow variations during the poststress recovery period, $[Ca^{2+}]_i$ measurements were continued after washout of *t*-BHP and drugs. During the first hour in

TABLE 2. Primers Used in RT-PCR for mRNA Expression Analysis

Gene	Gene bank accession no.	5′-primer	3′ primer	Product size (bp)
GFAP	L27219	1,434–1,453	1,808–1,827	394
GAPDH	NM_017008	1,455–1,474	1,514–1,532	78
R-AChE	AY555735	Same as T	189–206	98
T-AChE	BC094521	1,783–1,804	1,872–1,893	111
LVGCCA1C	M59786	2,623–2,642	2,861–2,881	259
LVGCCA1D	M57682	2,482–2,502	2,644–2,663	182
TRPM2	AY749166	2,424–2,443	2,509–2,528	104
CD11b	NM_012711	1,950–1,969	2,175–2,194	245

Primers were designed using the Primer3 program (Rozen and Skaletsky, 2000) and analyzed for structural anomalies and dimer formation using NetPrimer software (Premier Biosoft International, Palo Alto, USA). Then primer specificity was confirmed by comparison with DNA sequence databases using nucleotide–nucleotide BLAST (Available at: http://www.ncbi.nlm.nih.gov). Whenever possible, forward and reverse primers for each gene of interest were designed in separate exons to eliminate possible artifacts because of DNA contamination in RNA preps.

recovery, cumulative $[Ca^{2+}]_i$ levels in the different treatment groups converged (Figs. 4A,D), although the average rate of change in $[Ca^{2+}]_i$ remained high (Figs. 4B,E). Only control cells that had been exposed to verapamil displayed reduced cumulative and average ($P < 0.02$) $[Ca^{2+}]_i$ levels in both GH4 (Figs. 4D,E) and glial cells (Figs. 4A,B), despite the fact that verapamil appeared to have no effect on control astroglia $[Ca^{2+}]_i$ levels during the initial hour. Over the course of the subsequent 8 h, the average change in $[Ca^{2+}]_i$ gradually declined and all treatment groups were identical to controls (Figs. 4C,F), although astroglial $[Ca^{2+}]_i$ levels remained elevated as compared with initial values.

Oxidative Stress-Induced Changes in Gene Expression

We next investigated whether changes in AChE gene expression correlated with altered L-VGCC or TRPM2 expression. Specifics of primer design and sequences used in RT-PCR experiments are described in Table 2. RT-PCR analysis was performed in control and *t*-BHP-treated astroglia at 1, 4, and 24 h poststress (Fig. 5A). RT-minus controls were negative, indicating that there was no DNA contamination in the RNA preps. Gene expression in control cells did not change significantly throughout the recovery period. After *t*-BHP treatment, glial fibrillary acidic protein (GFAP), R-AChE, and TRPM2 mRNA were upregulated, while T-AChE, L-$VGCC_{A1C}$ ($Ca_V1.2$), and L-$VGCC_{A1D}$ ($Ca_V1.3$) expression decreased. GFAP expression was markedly increased within 4 h ($P < 0.001$) as compared with controls and remained elevated at 24 h ($P < 0.001$) poststress. Control astroglia expressed low levels of R-AChE and moderate levels of T-AChE. After *t*-BHP treatment, R-AChE increased by more than 5-fold ($P < 0.001$), whereas T-AChE expression decreased by 2-fold ($P < 0.05$). The induced increase in R-AChE mRNA peaked at 1 h, then slowly declined, approaching control levels by 24 h poststress. No evidence of TRPM2 expression was seen in control astroglia; however, after *t*-BHP exposure, a rapid but transient upregulation was observed. TRPM2 transcripts appeared within 1 h, peaked at 4 h ($P < 0.001$), and were diminished, but still apparent at 24 h poststress. L-$VGCC_{A1C}$ and L-$VGCC_{A1D}$ transcripts were abundant in control astroglia. However, after *t*-BHP

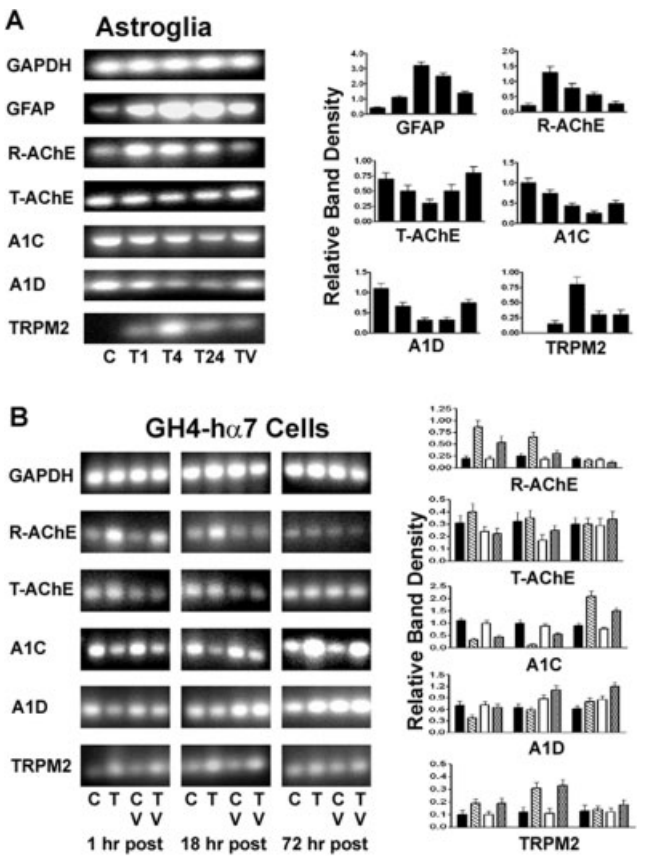

Fig. 5. RT-PCR analysis of gene expression in control and *t*-BHP stressed astroglia and GH4 cells: representative gel photographs and semiquantitative analysis. **A**: Gene expression in control astroglial cultures and in those treated for 1 h with 0.25 mM *t*-BHP or with 10 μM verapamil concurrent with *t*-BHP. Cells were recovered in serum-free medium for 1, 4, and 24 h poststress before extracting RNA for analysis. C = control astroglia, T1 = *t*-BHP-treated at 1 h poststress, T4 = *t*-BHP-treated at 4 h poststress, T24 = *t*-BHP-treated at 24 h poststress, TV = verapamil + *t*-BHP-treated at 24 h poststress. **B**: GH4 gene expression in control and 0.25 mM *t*-BHP treated cultures in the presence and absence of verapamil. RNA was extracted after 1, 18, or 72 h recovery from oxidative stress. C = control cells, T = *t*-BHP-treated, V = verapamil treatment. Relative band density measurements were obtained from three replicate experiments. Data is expressed as mean ± SEM.

treatment, both L-VGCC$_{A1C}$ and L-VGCC$_{A1D}$ transcript levels gradually declined in the initial 24 h poststress period to about 25% of control values ($P < 0.001$).

Verapamil application concurrent with *t*-BHP stress significantly inhibited upregulation of GFAP ($P < 0.01$) and R-AChE ($P < 0.05$) expression observed at 24 h poststress, but had no effect on TRPM2. The observed decrease in L-VGCC$_{A1D}$ expression in response to stress was also partially inhibited by verapamil treatment ($P < 0.02$). Although verapamil appeared to similarly mitigate downregulation of T-AChE and L-VGCC$_{A1C}$ expression in response to stress, the differences observed did not attain statistical significance ($P = 0.09$, $P = 0.06$ respectively).

Control GH4 cells expressed low levels of R-AChE and TRPM2, moderate levels of T-AChE, and high levels of GAPDH and L-VGCCs (Fig. 4B). No significant difference was observed in controls at 1, 18, or 72 h time points. Stress-induced changes in GH4 gene expression exhibited similar patterns to those seen in astroglia, in that R-AChE and TRPM2 were upregulated, while L-VGCCs were downregulated during the initial 24 h poststress. However, in contrast to astroglia, T-AChE expression remained relatively unchanged. R-AChE expression rapidly increased by 4-fold within 1 h ($P < 0.001$), remained significantly elevated at 18 h ($P < 0.01$), and returned to control levels by 72 h poststress. Significantly increased TRPM2 expression observed at 1 h poststress ($P = 0.05$) was still apparent and further increased at 18 h poststress ($P < 0.01$). L-VGCC$_{A1C}$ expression was reduced by 60% ($P < 0.001$) and L-VGCC$_{A1D}$ by 40% ($P < 0.05$) 1 h after *t*-BHP exposure. L-VGCC$_{A1C}$ transcripts remained suppressed at 18 h poststress ($P < 0.001$), whereas L-VGCC$_{A1D}$ expression had returned to control levels. However, at 72 h poststress, L-VGCC$_{A1C}$ expression was increased more than 2-fold ($P < 0.001$).

Verapamil treatment of unstressed GH4 cells had no significant effect on RNA expression at any of the time points tested. Co-application of verapamil with *t*-BHP treatment resulted in significant repression of *t*-BHP-induced upregulation of R-AChE at the 1 h ($P < 0.05$) and 18 h ($P < 0.05$) time points. In addition, verapamil treatment significantly mitigated stress-induced L-VGCC$_{A1C}$ downregulation at 18 h ($P < 0.05$) and upregulation at 72 h ($P < 0.01$) poststress. In contrast, verapamil exposure increased *t*-BHP-induced upregulation of L-VGCC$_{A1D}$ at 18 h ($P < 0.01$) and 72 h ($P < 0.05$) poststress. Neither T-AChE, nor TRPM2 expression, were significantly effected by verapamil treatment at any time point tested ($P > 0.05$).

To verify that the observed astroglial upregulation of TRPM2 mRNA was not an artefact caused by contamination of astroglial cultures by microglia, RT-PCR was performed using primers for TRPM2 and the cell type-specific markers GFAP (astrocytes) and CD11b (microglia). Whole rat brain RNA was used as a positive control; appropriate RT- and water controls were negative for amplification products. Cultured astroglia exposed to *t*-BHP for 1 h, then harvested for RNA extraction at 4 h poststress, displayed both GFAP and TRPM2, but no detectable CD11b expression (Fig. 6). In contrast, microglia expressed CD11b and TRPM2, but not GFAP.

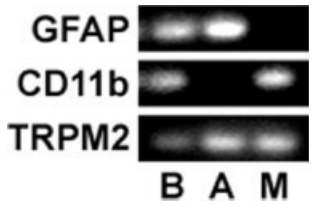

Fig. 6. RT-PCR analysis of cell type-specific markers and TRPM2 expression. B = rat brain, A = astrocyte culture treated with *t*-BHP and harvested at 4 h poststress, M = microglia culture.

Calcium Channel Modulation of Stress-Induced Changes in Global Protein Synthesis

Astroglial protein production was inhibited by almost 90% at 6 h poststress (Fig. 7A). This highly significant ($P < 0.0001$) reduction in new protein synthesis was not mitigated by blocking L-VGCC, or by inhibiting TRPM2 channel activation during exposure to stress conditions. In fact, the presence of verapamil during *t*-BHP exposure further depressed poststress protein synthesis by 20% as compared with *t*-BHP-stressed controls (Fig. 7A, inset graph); however, using the rigorous Bonferroni multiple comparison test, this difference failed to attain significance ($P = 0.08$). Although benzamide by itself had no significant effect on *t*-BHP-induced changes in protein synthesis, coapplication of verapamil and benzamide concurrent with *t*-BHP resulted in significant additional suppression of protein synthesis ($P < 0.01$) that was greater than was seen with verapamil alone.

Protein synthesis in astroglia remained suppressed 24 h after exposure to *t*-BHP as compared with controls ($P < 0.001$), but was increased 2-fold over levels observed at 6 h poststress (Fig. 7B). Recovery from initial protein synthesis inhibition was significantly enhanced in astroglia that had been exposed to calcium channel modulation during the period of oxidative stress. Glia stressed in the presence of nimodipine, or verapamil and DHBP, displayed double the amount of new protein synthesis as compared with those exposed to *t*-BHP alone ($P = 0.048$ and $P = 0.036$ respectively). Although verapamil treatment alone also enhanced protein synthesis by ~2-fold over *t*-BHP-induced levels, this increase was not statistically significant ($P = 0.089$). DHBP alone did not significantly alter *t*-BHP induced suppression of protein synthesis levels. As was seen at 6 h poststress, benzamide alone had no effect on *t*-BHP-induced inhibition of protein synthesis, whereas in combination with verapamil, or verapamil and DHBP, a highly significant effect on protein synthesis was observed when compared with *t*-BHP treated cells in the absence of drugs ($P < 0.007$ and $P < 0.001$ respectively).

At 72 h poststress a reversal of stress and drug effects was seen, with astroglial protein synthesis in stressed

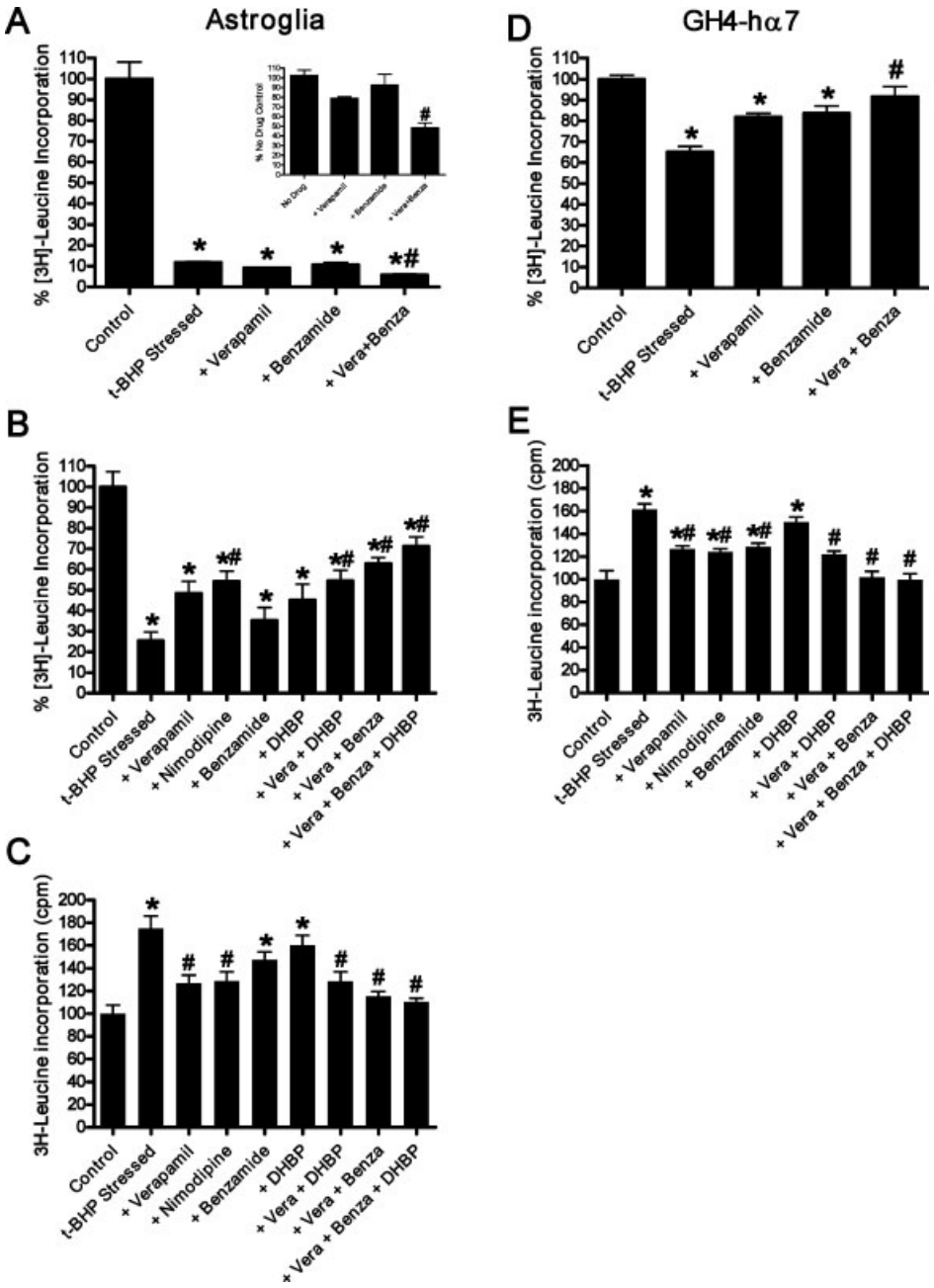

Fig. 7. Changes in protein synthesis in astroglia and GH4 cells in response to oxidative stress Cells were stressed for 1 h with 0.2 mM *t*-BHP in the absence and presence of various calcium channel modulators, then recovered in cell medium containing 15 μCi/mL [^{3}H]-leucine. Results are expressed as percent unstressed, no drug control values. Asterisks (*) indicate values significantly different from unstressed, no drug controls; (#) indicates values from cells stressed in presence of drugs that are significantly different from *t*-BHP-stressed controls. All experiments were performed in triplicate. **A**: Astroglia protein synthesis after 6 h recovery from oxidative stress. Inset graph illustrates drug effects on protein synthesis levels expressed as percent *t*-BHP-stressed, no drug controls. **B**: Astroglia protein synthesis after 24 h recovery. **C**: Astroglial protein synthesis after 72 h recovery. **D**: GH4 cell protein synthesis after 6 h recovery. **E**: GH4 cell protein synthesis after 24 h recovery.

cells significantly elevated ($P < 0.001$) over that observed in controls (Fig. 7C). Treatment with verapamil or nimodipine concurrent with *t*-BHP reduced the observed increase in protein synthesis ($P < 0.05$); however neither DHBP nor benzamide alone had a significant effect. Application of DHBP and benzamide in combination with verapamil did not further mitigate protein synthesis changes as compared with verapamil alone.

Similar findings were obtained with GH4 cells; however, protein synthesis changes were less sustained and the responses seen were less profound than those observed in astroglia. At 6 h poststress, protein synthesis was significantly suppressed in GH4 cells that had been exposed to *t*-BHP as compared with controls ($P = 0.006$, Fig. 7D). Neither verapamil, nor benzamide alone significantly changed the cellular responses to *t*-BHP-

induced oxidative stress, but when cells were treated with both verapamil and benzamide, stress-induced protein synthesis suppression was effectively abolished. Results in GH4 cells 24 h poststress were similar to those seen in astroglia at 72 h (Fig. 7E). Protein synthesis in stressed cells was increased ($P < 0.001$) over that observed in controls and DHBP had no effect on stress-induced changes. Cells that had been treated with verapamil ($P < 0.01$) or nimodipine ($P < 0.001$) during *t*-BHP-induced stress showed reduced protein levels as compared with *t*-BHP treated cells. In contrast with results in astroglia, benzamide significantly reduced GH4 cell protein synthesis at 24 h poststress ($P < 0.01$). Coapplication of benzamide with verapamil significantly reduced *de novo* protein synthesis as compared with verapamil alone ($P < 0.05$).

DISCUSSION

Although the role of astroglia in the progression of neurodegenerative disease is still relatively unknown, their importance in regulating the normal and abnormal neuronal environment is attracting increasing attention. Through calcium signaling cascades, astroglia control gene expression, neuronal differentiation, and programmed cell death, which are all integral to developmental and degenerative processes (Alberdi et al., 2005; Verkhratsky, 2006). Under conditions of oxidative stress, glial cells provide energy support for neurons, exert a protective function by scavenging and detoxifying ROS, and direct neuronal resistance or vulnerability to degeneration through calcium-dependent secretion of trophic or inflammatory factors (Morale et al., 2006).

In light of the importance of stress-induced glial calcium dysregulation in neurodegenerative processes (Alberdi et al., 2005; Mariani et al., 2005; Verkhratsky, 2006), we investigated the role of glial calcium channels in regulating transcriptional changes and release of a potential neurotrophic factor, AChE, in response to oxidative stress. To facilitate elucidation of the complex biological processes involved, we used cultured astrocytes and GH4-hα7 cells for comparative studies. Primary cortical astrocyte cultures are a well-documented standard model for measuring stress responses *in vitro* and provide consistent results which correlate well with results obtained *in vivo* (Gifford and Swanson, 2005; Hertz et al., 1998). GH4 cells, a rat pituitary tumor-derived cell line, are a proven system for studying mechanisms of intracellular calcium homeostasis and trophic factor release in secretory cells (Albert and Tashjian, 1984). The derivative GH4-hα7 cell line was chosen as a control for comparison with astroglia because preliminary experiments demonstrated that they release AChE in response to *t*-BHP-induced oxidative stress and express a full complement of cell surface receptors and ion channels important for the maintainance of calcium homeostasis by astroglia and neurons.

In this study, acute ROS exposure, comparable to oxidant levels measured *in vivo* in affected tissues in a rat model of stroke (up to 200 μM H_2O_2; Hyslop et al., 1995) and in neurodegenerative disease (reviewed in Butterfield, 2006; Chinopoulos and Adam-Vizi, 2001; Halliwell, 2006; Mariani et al., 2005; Polidori et al., 2007), produced sustained increases in $[Ca^{2+}]_i$, profound morphological changes, and increased AChE release in astroglia and GH4 cells. Elimination of $[Ca^{2+}]$ from the extracellular medium abolished induced phenotypic alterations and AChE release, while blockade of $[Ca^{2+}]$ entry via L-VGCC significantly diminished both effects. Whereas all calcium channel blockers tested reduced AChE release from unstressed astroglia, none had an effect on basal AChE release from control GH4 cells, suggesting that basal AChE release is differentially regulated in these cell types. In contrast, we show that, in both astroglia and GH4 cells, L-VGCCs predominantly control *t*-BHP-induced $[Ca^{2+}]$ influx and AChE release. Furthermore, in GH4 cells, benzamide inhibition of TRPM2 activation had an additive effect with L-VGCC blockers in reducing $[Ca^{2+}]$ influx during *t*-BHP exposure, but had no effect on poststress AChE release. These results indicate that, while basal AChE release is constitutive and nonspecific, induced AChE release is part of a generalized cellular response to oxidative stress specifically regulated by $[Ca^{2+}]$ influx through L-VGCC.

Previous reports investigating VGCC expression in cultured astrocytes yield conflicting results as to which alpha subunits they express (D'Ascenzo et al., 2004; LaTour et al., 2003). Most agree nevertheless that L-VGCC are not highly expressed by astrocytes under normal physiological conditions, but are upregulated in cultured and reactive astrocytes, and in pathological brain states. In this study, GH4 cells and reactive astroglia exhibited high expression of L-$VGCC_{A1C}$ and L-$VGCC_{A1D}$ mRNA, which initially decreased after exposure to oxidative stress, followed by a compensatory upregulation after 72 h. This finding is consistent with *in vivo* studies that demonstrated upregulation of L-$VGCC_{A1C}$ protein in astrocyte plasma membranes 7 day to 3 week after ischemia or brain injury (Chung et al., 2001; Westenbroek et al., 1998). However, in contrast to the results presented here and in a previous study (LaTour et al., 2003), these *in vivo* studies reported no evidence of L-$VGCC_{A1D}$ in astroglia, perhaps reflecting a significant difference between astrocytes in culture and those in a normal physiological environment.

Whereas other neuronal VGCCs (N,P/Q-type) mediate calcium-dependent synaptic vesicle fusion and neurotransmitter release, the primary function of L-VGCCs involves coupling of neuronal activity to gene transcription through $[Ca^{2+}]$ signaling cascades (Zhang et al., 2006). Consistent with that seen during neuronal differentiation (Luo et al., 1994), we found that upregulation of R-AChE expression in response to oxidative stress is mediated by $[Ca^{2+}]$ influx through L-VGCC. L-VGCC blockade with verapamil during *t*-BHP treatment resulted in partial suppression of R-AChE and GFAP upregulation, as well as stress-induced changes in L-$VGCC_{A1C}$ and L-$VGCC_{A1D}$ mRNA expression. Since L-VGCC blockade alone was not sufficient to abolish

induced AChE release or transcriptional changes, other factors, such as receptor-mediated signalling cascades, may be involved.

We also observed transient upregulation of TRPM2 RNA expression in response to oxidative stress in astroglia and in GH4 cells. A previous report (Kraft et al., 2004) cited evidence of weak TRPM2 mRNA expression in cultured astroglia, but the finding was attributed to microglial contamination of the cultures, since no functional response to ADP-ribose was observed. Although we cannot rule out the possibility that some microglia may have escaped detection, immunocytochemical analysis, and microscopic inspection indicate that our culture method produces 'pure' reactive astroglial cultures (Bond et al., 2006). In addition, RT-PCR analysis of samples for cell type specific markers confirmed the absence of microglia in astroglial cultures (Fig. 6). Moreover, TRPM2 expression in astroglia was detected only after exposure to oxidative stress, but not in control cultures, and both GH4 cells and astroglia displayed similar changes in TRPM2 expression patterns in response to *t*-BHP stimulation. These results indicate that reactive astroglia have the capacity to express TRPM2 under oxidative stress conditions.

Chuang et al. (2002) have demonstrated that oxidative stress induced by peroxides instigates upregulation of more than 60 genes within a few hours after treatment. Most notable among those overexpressed more than 2-fold were growth and transcription factors, DNA damage repair, anti-oxidant, and cAMP/Ca^{2+}-regulated genes. Interestingly, the transient changes we have observed in AChE and TRPM2 gene expression exhibited patterns of response similar to genes known to be modulated by the intermediate early genes c-fos and CREB. This observation is consistent with previous studies showing that [Ca^{2+}] influx via L-VGCC activates CREB (Dolmetsch et al., 2001; Zhang et al., 2006) and that rapid c-fos induction after exposure to acute stress precedes upregulation of R-AChE expression (Kaufer et al., 1998).

Whereas T-AChE expression is induced in many cells undergoing apoptosis (Zhang et al., 2002), preferential splicing for R-AChE is associated with stress responses (Pick et al., 2004) and neurotrophic effects (Luo et al., 1994). Oxidative stress-induced mitochondrial dysfunction, such as that seen in many neurodegenerative diseases (Andersen, 2004), can cause deficits in energy metabolism and increased formation of alternative splicing isoforms (Maracchioni et al., 2007). Thus the preferential upregulation of R- AChE may be a consequence of stress-induced mitochondrial alteration of polyribosome function. Such a mechanism would allow rapid production of a critical neurotrophic factor, while downregulating a pro-apoptotic molecule, to enhance neuronal survival under stress conditions without taxing limited cellular energy reserves. Similarly, the full transcript form of TRPM2 (TRPM2-L) specifically mediates apoptosis, whereas the alternatively spliced TRPM2-S inhibits apoptosis induced by oxidative stress (Fonfria et al., 2005). Since TRPM2 expression follows the same pattern as R-AChE, the observed increase in TRPM2 transcripts may represent a similar upregulation of the alternatively spliced anti-apoptotic isoform.

In addition to causing mitochondrial damage, oxidative stress and glial calcium dysregulation can exacerbate neurodegenerative processes through aberrant protein processing (McNaught et al., 2001; Shenton et al., 2006) and the formation of aggregated proteins (Butterfield and Kanski, 2001). Concommitent with AChE and TRPM2 RNA upregulation, we observed profound suppression of *de novo* protein synthesis after *t*-BHP treatment, followed by global upregulation of protein synthesis in astroglia and GH4 cells. These results are consistent with a recent study in yeast demonstrating increased mRNA transcription and polysome association and decreased translation initiation after exposure to peroxides (Shenton et al., 2006). Similar changes in astroglial protein synthesis after ischemia were shown to be essential to cell survival (Hori et al., 1994), suggesting that suppression of protein synthesis provides a protective effect by preventing translational errors under oxidative conditions. We also showed that the additive effects of L-VGCC blockade and TRPM2 inhibition during oxidative stress significantly enhanced recovery from protein synthesis suppression and repressed subsequent compensatory protein over-expression. These results indicate that calcium signaling is integral to astroglial transcriptional and translational responses to oxidative stress.

In conclusion, we have demonstrated that L-VGCCs expressed in reactive astroglia and GH4-hα7 cells, mediate ROS-induced [Ca^{2+}] influx and AChE release, alterations in AChE and calcium channel expression, and recovery from suppression of global protein synthesis (Fig. 8). In addition, we provide evidence that stress-induced changes in protein synthesis are also modified by TRPM2

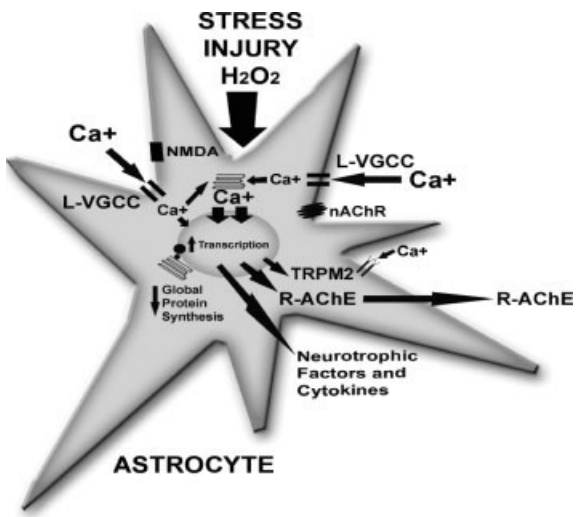

Fig. 8. Diagram summarizing the observed effects of oxidative stress on astroglia. Abbreviations: L-VGCC = L-type voltage-gated calcium channel, Ca^{+} = calcium ions, R-AChE = readthrough acetylcholinesterase isoform, TRPM2 = melastatin-like transient receptor potential 2, NMDA = *N*-methyl-D-aspartate receptor, nAChR = nicotinic acetylcholine receptor.

and report, for the first time, upregulation of TRPM2 calcium channel expression in astroglia in response to oxidative stress. There is mounting evidence that perturbed calcium homeostasis in glia plays a prominent role in the pathogenesis of neurodegenerative disease. Indeed, reactive astrogliosis has been recognized as the distinguishing feature characterizing both acute and chronic central nervous system damage in most degenerative pathologies (Marchetti et al., 2005). The data presented here highlights potential novel targets for interventive strategies in neurodegenerative disease. Moreover, these results reveal that through dynamic alterations oxidative stress initiates multiple calcium-regulated cascades in astroglia that operate in concert to allow rapid adaptation to the changing neuronal environment.

ACKNOWLEDGMENTS

GH4-hα7 cells were a gift from Merck & Co, Rahway, USA. Special thanks are due to Clive Garnham (Department of Pharmacology, Oxford University) for his technical assistance with calcium fluorescence assays.

REFERENCES

Albert PR, Tashjian AH. 1984. Relationship of thyrotropin-releasing hormone-induced spike and plateau phases in cytosolic free Ca^{2+} concentrations to hormone secretion. J Biol Chem 259:15350–15363.

Alberdi E, Sanchez-Gomez MV, Matute C. 2005. Calcium and glial cell death. Cell Calcium 38:417–425.

Andersen JK. 2004. Oxidative stress in neurodegeneration: Cause or consequence? Nat Med 10:S18–S25.

Bond CE, Patel P, Crouch L, Tetlow N, Day T, Abu-Hayyeh S, Williamson C, Greenfield SA. 2006. Astroglia up-regulate transcription and secretion of 'readthrough' acetylcholinesterase following oxidative stress. Eur J Neurosci 24:381–386.

Browne SE, Beal MF. 2006. Oxidative damage in Huntington's disease pathogenesis. Antioxid Redox Signal 8:2061–2073.

Butterfield DA. 2006. Oxidative stress in neurodegenerative disorders. Antioxid Redox Signal 8:1971–1973.

Butterfield DA, Kanski J. 2001. Brain protein oxidation in age-related neurodegenerative disorders that are associated with aggregated proteins. Mech Ageing Dev 122:945–962.

Chinopoulos C, Adam-Vizi V. 2001. Mitochondria deficient in complex I activity are depolarized by hydrogen peroxide in nerve terminals: Relevance to Parkinson's disease. J Neurochem 76:302–306.

Chuang YY, Chen Y, Gadisetti, Chandramouli VR, Cook JA, Coffin D, Tsai MH, DeGraff W, Yan H, Zhao S, Russo A, Liu ET, Mitchell JB. 2002. Gene expression after treatment with hydrogen peroxide, menadione, or t-butyl hydroperoxide in breast cancer cells. Cancer Res 62:6246–6254.

Chung YH, Shin C, Kim MJ, Cha CI. 2001. Enhanced expression of L-type Ca^{2+} channels in reactive astrocytes after ischemic injury in rats. Neurosci Lett 302:93–96.

Coleman BA, Taylor P. 1996. Regulation of acetylcholinesterase expression during neuronal differentiation. J Biol Chem 271:4410–4416.

D'Ascenzo M, Vairano M, Andreassi C, Navarra P, Azzena GB, Grassi C. 2004. Electrophysiological and molecular evidence of L-(Cav1), N-(Cav22), and R- (Cav23) type Ca^{2+} channels in rat cortical astrocytes Glia 45:354–363.

Day T, Greenfield SA. 2002. A non-cholinergic, trophic action of acetylcholinesterase on hippocampal neurons *in vitro*: Molecular mechanisms. Neuroscience 111:649–656.

Dolmetsch RE, Pajvani U, Fife K, Spotts JM, Greenberg ME. 2001. Signaling to the nucleus by an L-type calcium channel-calmodulin complex through the MAP kinase pathway. Science 294:333–339.

Dori A, Cohen J, Silverman WF, Pollack Y, Soreq H. 2005. Functional manipulations of acetylcholinesterase splice variants highlight alternative splicing contributions to murine neocortical development. Cereb Cortex 15:419–430.

Eimerl S, Schramm M. 1994. The quantity of calcium that appears to induce neuronal death. J Neurochem 62:1223–1226.

Ellman GL, Courtney KD, Andrea V, Featherstone RM. 1961. A new and rapid colorimetric determination of acetylcholinesterase activity. Biochem Pharmacol 7:88–95.

Fonfria E, Marshall IC, Benham CD, Boyfield I, Brown JD, Hill K, Hughes JP, Skaper SD, McNulty S. 2004. TRPM2 channel opening in response to oxidative stress is dependent on activation of poly(ADP-ribose) polymerase. Br J Pharmacol 143:186–192.

Fonfria E, Marshall IC, Boyfield I, Skaper SD, Hughes JP, Owen DE, Zhang W, Miller BA, Benham CD, McNulty S. 2005. Amyloid β-peptide(1-42) and hydrogen peroxide-induced toxicity are mediated by TRPM2 in rat primary striatal cultures. J Neurochem 95:715–723.

Gifford RG, Swanson RA. 2005. Ischemia-induced programmed cell death in astrocytes. Glia 50:299–306.

Greenfield SA, Vaux DJ. 2002. Parkinson's disease, Alzheimer's disease and motor neurone disease: Identifying a common mechanism Neuroscience 113:485–492.

Halliwell B. 2006. Oxidative stress and neurodegeneration: Where are we now? J Neurochem 97:1634–1658.

Hertz L, Peng L, Lai JCK. 1998. Functional studies in cultured astrocytes. Methods 16:293–310.

Hori O, Matsumoto M, Maeda Y, Ueda H, Ohtsuki T, Stern DM, Kinoshita T, Ogawa S, Kamada T. 1994. Metabolic and biosynthetic alterations in cultured astrocytes exposed to hypoxia/reoxygenation. J Neurochem 62:1489–1495.

Hyslop PA, Zhang Z, Pearson DV, Phebus LA. 1995. Measurement of striatal H_2O_2 by microdialysis following global forebrain ischemia and reperfusion in the rat: Correlation with the cytotoxic potential of H_2O_2 in vitro. Brain Res 671:181–186.

Kaufer D, Friedman A, Seidman S, Soreq H. 1998. Acute stress facilitates long-lasting changes in cholinergic gene expression. Nature 93:373–377.

Kraft R, Grimm C, Grosse K, Hoffmann A, Sauerbruch S, Kettenmann H, Schultz G, Harteneck C. 2004. Hydrogen peroxide and ADP-ribose induce TRPM2-mediated calcium influx and cation currents in microglia. Am J Physiol Cell Physiol 286:C129–C137.

LaTour I, Hamid J, Beedle AM, Zamponi GW, MacVicar BA. 2003. Expression of voltage-gated Ca^{2+} channel subtypes in cultured astrocytes. Glia 41:347–353.

Luo Z, Fuenica M, Taylor P. 1994. Regulation of acetylcholinesterase mRNA stability by calcium during differentiation from myoblasts to myotubes. J Biol Chem 44:27216–27223.

Maracchioni A, Totaro A, Angelini DF, Di Penta A, Bernardi G, Carri MT, Achsel T. 2007. Mitochondrial damage modulates alternative splicing in neuronal cells: Implications for neurodegeneration. J Neurochem 100:142–153.

Marchetti B, Kettenmann H, Streit WJ. 2005. Glia-neuron crosstalk in neuroinflammation, neurodegeneration, and neuroprotection. Brain Res Brain Res Rev 48:129–132.

Mariani E, Polidori MC, Cherubini A, Mecocci P. 2005. Oxidative stress in brain aging, neurodegenerative and vascular diseases: An overview. J Chromatogr B 827:65–75.

Markesbery WR, Lovell MA. 2006. DNA oxidation in Alzheimer's disease. Antioxid Redox Signal 8:2039–2045.

Mattson MP. 2006. Neuronal life-and-death signalling, apoptosis, and neurodegenerative disorders. Antioxid Redox Signal 8:1997–2006.

McNaught KS, Lee M, Hyun DH, Jenner P. 2001. Glial cells and abnormal protein handling in the pathogenesis of Parkinson's disease. Adv Neurol 86:73–82.

Morale MC, Serra PA, L'episcopo F, Tirolo C, Caniglia S, Testa N, Gennuso F, Giaquinta G, Rocchitta G, Desole MS, Miele E, Marchetti B. 2006. Estrogen, neuroinflammation and neuroprotection in Parkinson's disease: Glia dictates resistance versus vulnerability to neurodegeneration. Neuroscience 138:869–878.

Norris CM, Halpain S, Foster TC. 1998. Reversal of age-related alterations in synaptic plasticity by blockade of L-type Ca^{2+} channels. J Neurosci 18:3171–3179.

Pick M, Flores-Flores C, Soreq H. 2004. From brain to blood: Alternative splicing evidence for the cholinergic basis of Mammalian stress responses. Ann NY Acad Sci 1018:85–98.

Polidori MC, Griffiths HR, Mariani E, Mecocci P. 2007. Hallmarks of protein oxidative damage in neurodegenerative diseases: Focus on Alzheimer's disease. Amino Acids 32:553–559.

Porter JT, McCarthy KD. 1997. Astrocytic neurotransmitter receptors in situ and in vivo. Prog Neurobiol 51:439–455.

Rozen S, Skaletsky H. 2000. Primer3 on the WWW for general users and for biologist programmers. In: Krawetz S, Misener S, editors. Bioinformatics methods and protocols: Methods in molecular biology. Totowa NJ: Humana Press. pp 365–386.

Sharma KV, Koenigsberger C, Brimijoin S, Bigbee JW. 2001. Direct evidence for an adhesive function in the noncholinergic role of acetylcholinesterase in neurite outgrowth. J Neurosci Res 63:165–175.

Shenton D, Smirnova JB, Selley JN, Carroll K, Hubbard SJ, Pavitt GD, Ashe MP, Grant CM. 2006. Global translational responses to oxidative stress impact upon multiple levels of protein synthesis. J Biol Chem 281:29011–29021.

Shohami E, Gati L, Beit-Yannai E, Trembovler V, Kohen R. 1999. Closed head injury in the rat induces whole body oxidative stress: Overall reducing antioxidant profile. J Neurotrauma 6:365–376.

Sternfeld M, Shoham S, Klein O, Flores-Flores C, Evron T, Idelson GH, Kitsberg D, Patrick JW, Soreq H. 2000. Excess "read-through" acetylcholinesterase attenuates but the "synaptic" variant intensifies neurodeterioration correlates. Proc Natl Acad Sci USA 97:8647–8652.

Sultana R, Perluigi M, Butterfield DA. 2006. Protein oxidation and lipid peroxidation in brain of subjects with Alzheimer's disease: Insights into mechanism of neurodegeneration from redox proteonomics. Antioxid Redox Signal 8:2021–2037.

Vaca K, Wendt E. 1992. Divergent effects of astroglial and microglial secretions on neuron growth and survival. Exp Neurol 118:62–72.

Verkhratsky A. 2006. Glial calcium signalling in physiology and pathophysiology. Acta Pharmacol Sin 27:773–780.

Verkhratsky A, Orkland RK, Kettenmann H. 1998. Glial calcium: Homeostasis and signalling function. Physiological Rev 78:99–141.

Westenbroek RE, Bausch SB, Lin RCS, Franck JE, Noebels JL, Catterall WA. 1998. Upregulation of L-type Ca^{2+} channels in reactive astrocytes after brain injury, hypomyelination, and ischemia. J Neurosci 18:2321–2334.

Whyte KA, Greenfield SA. 2003. Effects of acetylcholinesterase and butyrylcholinesterase on cell survival, neurite outgrowth, and voltage-dependent calcium currents of embryonic ventral mesencephalic neurons. Exp Neurol 184:496–509.

Zhang H, Fu Y, Altier C, Platzer J, Surmeier DJ, Bezprozvanny I. 2006. $Ca_V1.2$ and $Ca_V1.3$ neuronal L-type calcium channels: Differential targeting and signalling to pCREB. Eur J Neurosci 23:2297–2310.

Zhang XJ, Yang L, Zhao Q, Caen JP, He HY, Jin QH, Guo LH, Alemany M, Zhang LY, Shi YF. 2002. Induction of acetylcholinesterase expression during apoptosis in various cell types. Cell Death Differ 9:790–800.